ADVANCED OPTICAL MATERIALS
www.advopticalmat.de

The Effect of the Relative Size of the Exciton Reservoir on Polariton Photophysics

*Rahul Bhuyan, Maksim Lednev, Johannes Feist, and Karl Börjesson**

Strong interactions between excitons and photons lead to the formation of exciton-polaritons, which possess different properties compared to their constituents. Polaritons are created by incorporating a dye in an optical cavity where the electromagnetic field is tightly confined. The interest in the subject has exploded in recent years due to the ability to change (photo)chemistry, but still as simple a variable as the yield of emission varies between studies. For the field to progress, linking observables to system parameters is a dire need. Here, the study pairs emission yield to the size of the so-called exciton reservoir, which dictates polariton relaxation dynamics. To do this, a method is devised to experimentally control the relative size of the exciton reservoir and link it to the yield of emission. Thus, the results enable comparison of the photophysics of previous studies within the field and provide the tools to study the effect of the exciton reservoir on polariton photochemistry.

1. Introduction

Organic chemistry can produce close to any molecule we can imagine, and fine-tuning of the molecular structure is a regular practice to achieve desirable properties. However, structural fine-tuning is time-consuming, and the laws of physics may still be a limitation. An alternative approach to tailoring molecular properties is provided by strong coupling of a molecular transition to an electromagnetic field.[1] Strong coupling has gathered considerable attention in recent years because it has been shown to modify photochemical[2] and chemical reactivity,[3] enable long-distance energy transfer,[4] promote reverse intersystem crossing,[5] affect singlet fission and triplet-triplet annihilation,[6] facilitate room temperature BEC,[7] and enhance organic electronics.[8] Still, despite these advancements, even basic photophysical properties are not comparable between studies. For instance, the emission quantum yield and emission lifetime have been shown to be smaller, the same, or higher in the strong compared to the weak coupling regime.[9]

For an organic dye, relaxation from higher excited states to the lowest vibrational level of the first excited state is very fast. However, in the strong coupling regime, relaxation kinetics is quite different due to the so-called exciton reservoir. The exciton reservoir is also often denoted as the dark states and should not be confused with uncoupled molecules, which are molecules that do not couple to the cavity mode of interest (for instance by being placed at nodes of the electromagnetic field or having a transition dipole moment oriented in an orthogonal direction to the electromagnetic field). In the strong coupling regime, an in-resonance transition dipole moment of the dyes collectively couples to a cavity mode (**Figure 1**a). When N molecules are coupled to the cavity mode, $N+1$ new eigenstates are formed.[10] Two of these states gain all oscillator strength. These are called the upper (UP) and lower (LP) polaritons, which are separated in energy by the Rabi splitting. The remaining $N-1$ states are optically inactive with an energy similar to the envelope of the molecular absorption.[11] These states are known as the exciton reservoir and regulate the photochemistry and photophysics. The polaritonic states are delocalized over the N molecules taking part in the hybridization, but each state of the exciton reservoir is localized over barely more than a single molecule.[4b,c] As a result, the rate of transitions between a state in the exciton reservoir and a polariton is reduced with one over N due to a wavefunction overlap mismatch.[11a] The large number (N-1) of states in the exciton reservoir compensates for the wavefunction overlap mismatch in the transition from the UP to the exciton reservoir. However, relaxation from the exciton reservoir to the LP is slow due to a lack of such compensation in LP. Furthermore, the relaxation from the LP to the ground state through photon leakage through the mirrors is fast in typical experimental setups. Excited state dynamics therefore mainly depend upon the relaxation from the exciton reservoir to the LP, which depends on the size of the exciton reservoir (N). Still, there is no experimental study on how the photophysics of polaritons is affected by the relative size of N. This is despite the exciton reservoir being identified as a major factor in all theoretical models within this research field.

R. Bhuyan, K. Börjesson
Department of Chemistry and Molecular Biology
University of Gothenburg
Kemivägen 10, Gothenburg 41296, Sweden
E-mail: karl.borjesson@gu.se

M. Lednev, J. Feist
Departamento de Física Teórica de la Materia Condensada and Condensed Matter Physics Center (IFIMAC)
Universidad Autónoma de Madrid
Madrid 28049, Spain

The ORCID identification number(s) for the author(s) of this article can be found under https://doi.org/10.1002/adom.202301383

DOI: 10.1002/adom.202301383

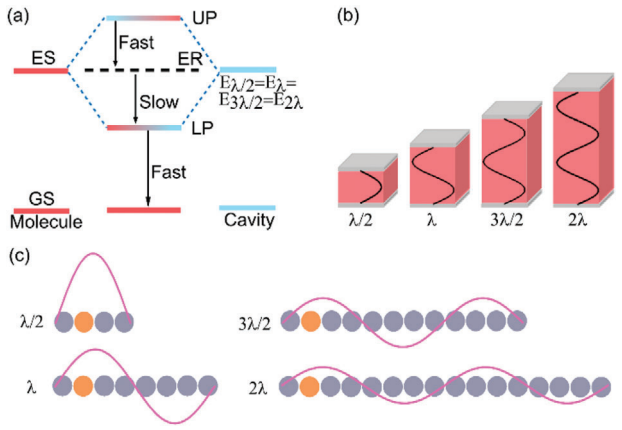

Figure 1. a) Jablonski diagram of the interaction of a molecular transition and cavity modes (different cavity mode order $\lambda/2$, λ, $3\lambda/2$, and 2λ) having the same cavity energy, resulting in the formation of two new hybrid states, the upper (UP) and lower (LP) polaritons, and N-1 states having the same energy as the molecular excited state, that is the exciton reservoir (ER). Here GS and ES represent the ground and excited states of the molecular transition. The relaxation from UP to ER is fast compared to ER to LP and LP to GS relaxations. The relaxation dynamics mainly depend upon the rate of the transition from ER to LP. b) Pictorial representation of $\lambda/2$, λ, $3\lambda/2$, and 2λ mode order cavities having the same cavity energy. c) Pictorial representation of the wavefunction overlap between the LP and the exciton reservoir. The purple wavefunction represents the delocalized polaritonic state. The spheres represent individual molecules coupled to the cavity mode (exciton reservoir) and the orange sphere represents the excited state in the exciton reservoir from which energy is transferred to the polaritonic state.

Here, we provide experimental evidence on how the size of the exciton reservoir affects the polariton photophysics. We start with devising a method to control the size of the exciton reservoir. We then continue by showing that the magnitude of energy relaxation toward the emissive LP follows the inverse of this size. We further show how the polariton emission efficiency is affected by the cavity energy. We hope that our findings will enable a better comparison of photochemistry and photophysics in the strong coupling regime of past, present, and future studies.

2. Results and Discussion

To probe the effect of the number of molecules coupled to a cavity mode (N) on polariton photophysics, one needs to have a method to control N. The below-described method assumes a cavity with ideal reflectors (negligible penetration of the electromagnetic field into the mirrors) that contains dyes that are homogenously distributed from mirror to mirror. The number of molecules per cavity mode can be represented by,

$$N = \frac{n}{N_{\mathrm{ph}}} \tag{1}$$

where n is the 2D projected density of molecules inside the optical cavity, and N_{ph} is the 2D density of cavity modes. For dyes homogeneously distributed in an optical cavity, the 2D projected density of molecules, n, is simply the 3D density times the cavity length L_{cav}. The density of cavity modes for the m^{th} mode order can be represented by,[11b]

$$N_{\mathrm{ph}}^{m} = \frac{n_{\mathrm{eff}}^2}{4\pi c^2 \hbar^2}\left(E_{\mathrm{c},m}^2\left(k_{\parallel,\mathrm{max}}\right) - E_{\mathrm{c},m}^2\left(0\right)\right) \tag{2}$$

where $E_{\mathrm{c},m}(k_{\parallel,\mathrm{max}})$ is the cavity energy at the maximum in-plane momentum, $E_{\mathrm{c},m}(0)$ is the minimum ($k_{\parallel} = 0$) cavity energy for m^{th} cavity mode order, n_{eff} is the refractive index, c is the speed of light, and $\bar{h}$ is the reduced Plank´s constant. The energy of the m^{th} cavity mode order is given by,

$$E_{\mathrm{c},m}\left(k_{\parallel}\right) = \frac{\hbar c}{n_{\mathrm{eff}}}\sqrt{k_{\parallel}^2 + \left(\frac{m\pi}{L_{\mathrm{cav}}}\right)^2} \tag{3}$$

$$k_{\parallel} = \frac{2\pi}{\lambda}\sin\theta \tag{4}$$

where L_{cav} is the thickness of the cavity, $k_{\parallel}$ is the in-plane momentum, θ is the angle of incidence, and λ is the wavelength of the incident light. By keeping L_{cav}/m constant, it is thus possible to make cavities with identical dispersion relations $E_{\mathrm{c},m}(k_{\parallel})$ (for different mode orders), and thus to maintain the same cavity mode density N_{ph}. At the same time, the 2D density of molecules scales with L_{cav}. The number of molecules per photonic mode, N, thus can be varied by changing the cavity mode order while adjusting the cavity length accordingly to keep L_{cav}/m constant. At the same time, the Rabi splitting is maintained since it depends on the 3D molecule density and is thus independent of L_{cav}. This allows the effect of N on the photophysics of polaritons to be probed by comparing cavities with different mode orders, maintaining a fixed cavity energy and polariton dispersion. Furthermore, a simple pictorial view can be given to the theoretical description above. With increasing mode order, a decrease in the wavefunction overlap between the exciton reservoir and the lower polariton can be expected (Figure 1b,c). Thus, giving a reduced rate of the transition as per the Fermi golden rule. We note that this argument applies both to vibration-assisted relaxation and radiative pumping mechanisms from the reservoir to the LP.[4b,c]

2.1. Setup for the Study

To understand how the relative number of molecules coupled to a cavity mode affects the polaritonic emission, cavities having different cavity mode orders ($\lambda/2$, λ, $3\lambda/2$, and 2λ) but a constant cavity mode energy is needed (Figure 1b). Cavities were fabricated on clean glass substrates, on which first a thick Ag mirror was sputtered. Afterward, a dye film was deposited, followed by the sputtering of a second thin, semitransparent Ag mirror. Different mode orders can be achieved by varying the cavity thickness, which thus can be achieved by varying the dye film thickness. Furthermore, the concentration of the dye should be the same irrespective of thickness of the films for the previous theoretical reasoning to be valid. To keep a constant dye concentration as well as to get access to thick films, evaporation is preferred over spin coating of the dye films (this is because of the limited solubility of organic dyes that constrains the film thickness when spin coating). Thus, an evaporable dye is needed, with a large enough

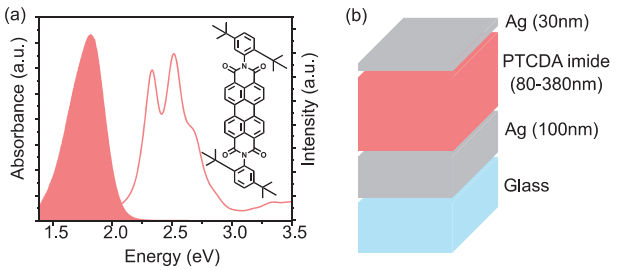

Figure 2. a) Solid-state absorption (red curve) and emission (red fill) spectra together with the molecular structure of *N*,*N*-bis(2,5-diter–butylphenyl)−3,4,9,10-perylenedicarboximide (PTCDA Imide). b) Cavity structure from top to bottom: Ag (30 nm), PTCDA imide film (80–380 nm), Ag (100 nm), glass substrate.

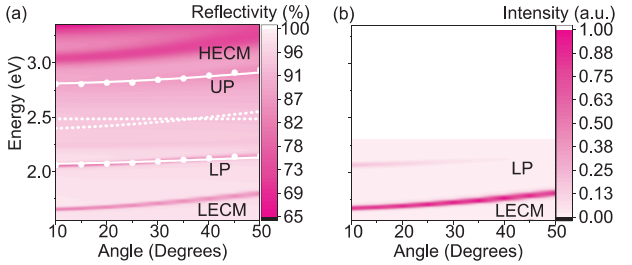

Figure 3. Photophysical measurements of one of the studied cavities with a mode order of 2λ and a cavity energy ($E_{c,4}(0)$) of 2.391 eV. a) Angle-dependent reflectivity of the cavity. Solid circles represent experimental polaritonic peaks, solid lines correspond to the fitting of the LP and UP using the coupled harmonic oscillator model, and dotted lines correspond to excitonic and cavity energies. The band at 3.03 eV is a higher order cavity mode (HECM), the band at 1.7 eV is a lower energy cavity mode (LECM), and the onset of absorption of the Ag mirrors can be seen at 3.3 eV. b) Angle-dependent emission when exciting the UP (443 nm).

transition dipole moment to allow reaching the strong coupling regime.

We choose the evaporable molecule *N*,*N*-bis(2,5-diter-butyl phenyl)−3,4,9,10-perylene dicarboximide (PTCDA imide) for this study. **Figure 2**a displays the solid-state absorption (red curve) and emission spectra (red fill), and the molecular structure for this molecule. PTCDA imide has three absorption peaks, at 2.327, 2.510, and 2.670 eV, which most likely correspond to three vibronic states for the same electronic transition. The emission spectrum of a solid-state PTCDA imide film is Gaussian-shaped and centered at 1.82 eV. There is no obvious emission from trap states, such as excimers or H/J-aggregates, despite the high concentration of the dye. The chosen organic molecule, PTCDA imide, is thus well-behaved in the solid state and fulfills all the requirements for this study.

2.2. Entering the Strong Coupling Regime

Using PTCDA imide and Ag mirrors, optical cavities having quality factors of roughly 20–25 could successfully be made (Table S1, Supporting Information). Twenty cavities were fabricated by varying the thickness of the molecular film. This created a spectrum of cavity mode orders ($\lambda/2$, λ, $3\lambda/2$, and 2λ), and cavity energies coupled to the lowest energy electronic transition of PTCDA imide. The angle-dependent reflectivity of all cavities (**Figure 3**a; Figures S2–S5, Supporting Information) were recorded to verify that the strong coupling regime is reached and to extract the cavity energies at $k_{\|} = 0$ and the coupling strengths (V_a). The angle-dependent reflectivity of all cavities were fitted using a coupled harmonic oscillator model.[12]

$$E_{\mathrm{UP/LP}}\left(k_{\|}\right) = \frac{1}{2}\left(E_x + E_{c,m}\left(k_{\|}\right)\right) \pm \sqrt{V_a^2 + \frac{1}{4}\left(E_x - E_{c,m}\left(k_{\|}\right)\right)^2} \quad (5)$$

where E_{UP} and E_{LP} are the energies of the upper- and lower polaritons, respectively, E_x is the exciton energy (which is independent of $k_{\|}$), which was calculated by the weighted average of the three absorption peaks (2.486 eV; see Section S2.1 and Table S4, Supporting Information for details). The fit was performed globally for all cavities at the same time, with cavity thicknesses (L_{cav}) and coupling strengths (V_a) as individual parameters per cavity, while the refractive index (n_{eff}) was treated as a global parameter. All fitting parameters are given in Table S2 (Supporting Information).

The Rabi splitting ($2V_a$) of the cavities varies from 714 to 738 meV. This is considerably larger than the average of the full-width half maxima of the molecular transition (456 meV) and of the cavity mode (120–135 meV), showing that the cavities are unambiguously in the strong coupling regime. The coupling strength is considerable in comparison to the exciton energy ($V_a/E_x = 15\%$), such that the systems are even in the ultrastrong coupling regime. Furthermore, the coupling strength (V_a) is close to constant as expected, and independent of the cavity mode order and cavity energy (Figure S6, Supporting Information).

2.3. Angle Dependent Photoluminescence

For the cavities chosen, the size of the exciton reservoir depends on the cavity mode order. By observing the LP emission intensity when exciting the UP, the yield in the relaxation pathways from the UP, via the exciton reservoir, to the LP can be examined. Relaxation from the UP to the exciton reservoir is expected to be fast and efficient due to the large number of final states (Figure 1). On the other hand, relaxation from the exciton reservoir to the LP is slow and inversely varies with the size of the exciton reservoir.[11,13] The quantum yield of emission of the used dye is low, such that the deexcitation from the reservoir is dominated by non-radiative decay. In this regime, the yield of polariton emission scales directly with the rate of the transition from the exciton reservoir to the LP, $QY = k_{\mathrm{ER}\rightarrow\mathrm{LP}}/k_{\mathrm{tot}} \approx k_{\mathrm{ER}\rightarrow\mathrm{LP}}/k_{\mathrm{nonrad}}$ (where k_{nonrad} relates to the non-radiative rate from the exciton reservoir to the ground state). By observing the emission intensity of cavities with varying cavity mode order and cavity energy, conclusions on the relative size of the exciton reservoir can thus be made.

We perform steady-state emission experiments and the angle-dependent photoluminescence of all the cavities was measured by exciting the UP at an angle of 15 degrees normal to the cavity surface. The angle-resolved emission was measured in the plane orthogonal to the excitation, to avoid specular reflection into the

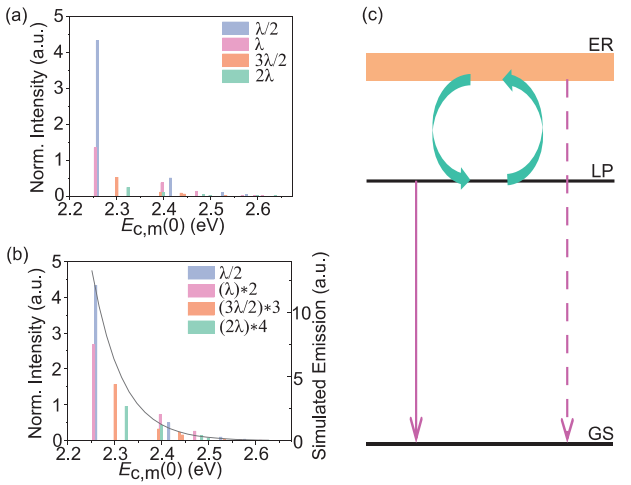

Figure 4. Polaritonic emission of cavities. a) Bar diagram of absorption normalized integrated polaritonic emission of cavities at 10 degrees normal to the cavity surface. b) Bar diagram of (mode order* absorption normalized integrated polariton emission at 10 degrees normal to the cavity surface). The brown curve shows simulated emission efficiency from the model schematically represented in inset (c). c) Simplistic kinetic model of lower polaritonic emission (for details see Section S2.3, Supporting Information).

detector. The emission from the LP was extracted by fitting a Gaussian function to the LP part of the cavity emission (Section S2.2, Supporting Information). The emission intensity was normalized by the absorbance at the excitation wavelength. All cavities were modeled using the transfer matrix method (Section S1.4 and Figures S7–S11, Supporting Information),[14] which was used to extract the absorbance from only the dye film (thus excluding the absorbance contribution from the Ag mirrors). Finally, the normalized polaritonic emission was integrated over the energy of emission in eV scale and plotted as a function of cavity energy at $k_{\|} = 0$ (**Figure 4**a). We note that polaritonic emission is independent of the coupling strength (Figure S12, Supporting Information).

Two trends are evident in the polariton emission intensity. 1) The polaritonic emission decreases in relation to an increase in cavity mode order in the cavities while maintaining a fixed cavity energy ($E_{c,m}(0)$). This is in line with expectations (see theoretical discussion above). To further analyze the integrated polaritonic emission, it was multiplied by the cavity mode order (Figure 4b). Now, cavities with similar cavity energy ($E_{c,m}(0)$), also have similar integrated polaritonic emission, irrespective of cavity mode order. This implies that the yield of polaritonic emission inversely varies with the cavity mode order. The size of the exciton reservoir directly varies with the cavity mode order (Equation (1)). Thus, indicating that the polaritonic emission (due to the rate of relaxation from the exciton reservoir to the LP) inversely varies with the size of the exciton reservoir, maintaining fixed cavity energy. 2) The LP emission decreases with an increase in the cavity energy ($E_{c,m}(0)$) when maintaining a fixed cavity mode order. To capture this emission intensity variation, we use a simplistic kinetic model that is still able to capture the trends in the emission intensity (Figure 4c; Section S2.3, Supporting Information). The model includes only two states (the exciton reservoir and LP), where a competition between non-radiative relaxation from the exciton reservoir and radiative relaxation from the LP occurs. The model does not explicitly include entropy effects, which from a statistical thermodynamics perspective significantly contribute to the free energy due to the large difference in the number of states between the LP and the exciton reservoir.[15] Instead, these effects are represented by the increased value of the rate from the LP to the exciton reservoir in the model. In short, by decreasing the cavity energy, the rate of polaritonic emission increases due to a larger photonic fraction of the polariton. Simultaneously, the rate of transfer from the polaritonic state to the exciton reservoir decreases due to a larger energy separation making this transfer more endothermic. These two effects work in conjunction to favor the relaxation pathway toward polaritonic emission.

2.4. Further Analysis of Secondary Emission

It is interesting to further analyze an unexpected but typical feature of the recorded emission spectra (Figure 3b; Figures S4 and S5, Supporting Information). In addition to the polaritonic emission (at 2.0–2.2 eV), a secondary low-energy emission band (at 1.6–1.8 eV) was observed. This low energy emission is prominent in higher order cavities ($3\lambda/2$, and 2λ) and has the same energy as a low energy cavity mode (at 1.6–1.8 eV in Figure 3a). A comparison of the magnitude of the polaritonic emission and the low energy emission is shown in Figure S15 (Supporting Information). To examine the origin of the low energy emission, we multiplied the absorption of the active layer of the cavity by the molecular emission (Figure S13, Supporting Information). The resulting filtered emission through the cavity is similar to the observed emission. It implies that the low-energy emission occurs due to radiative pumping from the exciton reservoir through this low-energy cavity mode. The question then arises if this low-energy cavity mode can be thought of as fully uncoupled, or if it is also affected by coupling to the cavity mode. In the high mode order cavities where low energy emission is prominent, transfer matrix calculations show a shift in the energy of these low-energy modes with and without dyes present (Figures S10 and S11, Supporting Information), thus indicating a small contribution from multimode coupling, including one strongly and one weakly coupled cavity mode. The nature of the lower energy mode was further explored by fitting the reflectivity data with a coupled harmonic oscillator model containing 1 exciton and 2 cavity modes (Figure S16, Supporting Information). The Hopfield coefficients for the low emission mode were nearly completely photonic, further corroborating the view of this mode to be practically uncoupled (but not far off to be coupled). As the 2λ cavity is on the onset of multimode coupling, it is the longest cavity for the used molecular system where the independence between coupling strength and cavity mode is expected. Generally, which cavity mode that forms this limit is system-specific as it depends on the exciton energy and Rabi splitting.

3. Conclusion

Here, we rationalize why the emission yield in the strong coupling regime varies in different circumstances. We start by showing that the relative size of the so-called exciton reservoir scales

linearly with the cavity mode order. A large number of cavities containing a PTCDA imide derivative was made, all having different cavity mode order and cavity energy. These were shown to couple strongly with the S_1 transition of the PTCDA derivative, and their relative emission intensity was recorded. For the same cavity energy, the relative emission scales inversely with the cavity mode order. The size of the exciton reservoir scale linearly with the cavity mode order and dictates the rate of transfer to the emissive LP state, which is rate limiting. Thus, a method for controlling the effect of the exciton reservoir on the polaritonic dynamics is found. From a polariton photochemistry perspective, this effect can be used to tune the reaction pathway. With a low mode order, the dynamical equilibrium between the LP and the exciton reservoir is relatively shifted toward the LP as compared to when a higher mode order cavity is used. Low mode order cavities are therefore preferable when observing photochemistry happening from the lower polariton branch, and high mode order cavities are preferable when observing photochemistry occurring from the exciton reservoir. The relative yield of emission was further seen to depend on the cavity energy. This observation could be rationalized by a very simplistic two-state model. The field of polaritonic chemistry can be regarded to still be in its infancy since as simple an observable as the emission yield has varied between studies. We show here how the yield of emission changes as a function of cavity mode order and energy, thus linking the observed photophysics to the size of the exciton reservoir. We hope that these findings will enable a better comparison between past, present, and future studies, and inspire new investigations on the effect of the size of the exciton reservoir on polaritonic chemistry.

Supporting Information

Supporting Information is available from the Wiley Online Library or from the author.

Acknowledgements

K.B. gratefully acknowledges the financial support from the Swedish Research Council (2020-03578) and the European Research Council (ERC-2017-StG-757733). M.L. and J.F. gratefully acknowledge support by the Spanish Ministry of Science and Innovation - Agencia Estatal de Investigación/10.13039/501100011033 through grants PID2021-125894NB-I00, CEX2018-000805-M (through the María de Maeztu program for Units of Excellence in R&D), and PRE2021-098978 (to M.L. with support from ESF+), and from the European Research Council through grant ERC-2016-StG-714870.

Conflict of Interest

The authors declare no conflict of interest.

Data Availability Statement

The data that support the findings of this study are available from the corresponding author upon reasonable request.

Keywords

polariton photophysics, rabi splitting, relaxation dynamics, strong exciton-photon coupling

Received: June 12, 2023
Revised: August 14, 2023
Published online: October 15, 2023

[1] a) T. W. Ebbesen, *Acc. Chem. Res.* **2016**, *49*, 2403; b) S. Haroche, D. Kleppner, *Phys. Today* **1989**, *42*, 24; c) M. Hertzog, M. Wang, J. Mony, K. Borjesson, *Chem. Soc. Rev.* **2019**, *48*, 937; d) D. G. Lidzey, D. D. C. Bradley, M. S. Skolnick, T. Virgili, S. Walker, D. M. Whittaker, *Nature* **1998**, *395*, 53; e) M. Ruggenthaler, N. Tancogne-Dejean, J. Flick, H. Appel, A. Rubio, *Nat. Rev. Chem.* **2018**, *2*, 390; f) P. Torma, W. L. Barnes, *Rep Prog Phys* **2015**, *78*, 013901.

[2] a) T. Schwartz, J. A. Hutchison, C. Genet, T. W. Ebbesen, *Phys. Rev. Lett.* **2011**, *106*, 196405; b) J. Mony, C. Climent, A. U. Petersen, K. Moth-Poulsen, J. Feist, K. Börjesson, *Adv. Funct. Mater.* **2021**, *31*, 2010737; c) J. A. Hutchison, T. Schwartz, C. Genet, E. Devaux, T. W. Ebbesen, *Angew. Chem., Int. Ed.* **2012**, *51*, 1592.

[3] A. Thomas, J. George, A. Shalabney, M. Dryzhakov, S. J. Varma, J. Moran, T. Chervy, X. Zhong, E. Devaux, C. Genet, J. A. Hutchison, T. W. Ebbesen, *Angew. Chem., Int. Ed.* **2016**, *55*, 11462.

[4] a) K. Georgiou, R. Jayaprakash, A. Othonos, D. G. Lidzey, *Angew. Chem., Int. Ed.* **2021**, *60*, 16661; b) X. L. Zhong, T. Chervy, L. Zhang, A. Thomas, J. George, C. Genet, J. A. Hutchison, T. W. Ebbesen, *Angew. Chem., Int. Ed.* **2017**, *56*, 9034; c) D. M. Coles, N. Somaschi, P. Michetti, C. Clark, P. G. Lagoudakis, P. G. Savvidis, D. G. Lidzey, *Nat. Mater.* **2014**, *13*, 712; d) M. Du, L. A. Martinez-Martinez, R. F. Ribeiro, Z. Hu, V. M. Menon, J. Yuen-Zhou, *Chem. Sci.* **2018**, *9*, 6659; e) K. Georgiou, P. Michetti, L. Z. Gai, M. Cavazzini, Z. Shen, D. G. Lidzey, *ACS Photonics* **2018**, *5*, 258; f) S. C. Hou, M. Khatoniar, K. Ding, Y. Qu, A. Napolov, V. M. Menon, S. R. Forrest, *Adv. Mater.* **2020**, *32*, 2002127.

[5] a) Y. Yu, S. Mallick, M. Wang, K. Borjesson, *Nat. Commun.* **2021**, *12*, 3255; b) E. Eizner, L. A. Martinez-Martinez, J. Yuen-Zhou, S. Kena-Cohen, *Sci. Adv.* **2019**, *5*, eaax4482; c) K. Stranius, M. Hertzog, K. Borjesson, *Nat. Commun.* **2018**, *9*, 2273.

[6] a) B. Liu, V. M. Menon, M. Y. Sfeir, *ACS Photonics* **2020**, *7*, 2292; b) L. A. Martinez-Martinez, M. Du, R. F. Ribeiro, S. Kena-Cohen, J. Yuen-Zhou, *J. Phys. Chem. Lett.* **2018**, *9*, 1951; c) A. M. Berghuis, A. Halpin, L. V. Quynh, M. Ramezani, S. J. Wang, S. Murai, J. G. Rivas, *Adv. Funct. Mater.* **2019**, *29*, 1901317; d) D. Polak, R. Jayaprakash, T. P. Lyons, L. A. Martinez-Martinez, A. Leventis, K. J. Fallon, H. Coulthard, D. G. Bossanyi, K. Georgiou, A. J. Petty Ii, J. Anthony, H. Bronstein, J. Yuen-Zhou, A. I. Tartakovskii, J. Clark, A. J. Musser, *Chem. Sci.* **2020**, *11*, 343; e) C. Ye, S. Mallick, M. Hertzog, M. Kowalewski, K. Borjesson, *J. Am. Chem. Soc.* **2021**, *143*, 7501.

[7] a) J. D. Plumhof, T. Stoferle, L. Mai, U. Scherf, R. F. Mahrt, *Nat. Mater.* **2014**, *13*, 247; b) J. Tang, J. Zhang, Y. Lv, H. Wang, F. F. Xu, C. Zhang, L. Sun, J. Yao, Y. S. Zhao, *Nat. Commun.* **2021**, *12*, 3265.

[8] a) C. Bujalance, V. Esteso, L. Calio, G. Lavarda, T. Torres, J. Feist, F. J. Garcia-Vidal, G. Bottari, H. Miguez, *J. Phys. Chem. Lett.* **2021**, *12*, 10706; b) C. A. DelPo, S. U. Z. Khan, K. H. Park, B. Kudisch, B. P. Rand, G. D. Scholes, *J. Phys. Chem. Lett.* **2021**, *12*, 9774; c) E. Eizner, J. Brodeur, F. Barachati, A. Sridharan, S. Kena-Cohen, *ACS Photonics* **2018**, *5*, 2921; d) A. Mischok, J. Luttgens, F. Berger, S. Hillebrandt, F. Tenopala-Carmona, S. Kwon, C. Murawski, B. Siegmund, J. Zaumseil, M. C. Gather, *J. Chem. Phys.* **2020**, *153*, 201104; e) M. Wang, M. Hertzog, K. Borjesson, *Nat. Commun.* **2021**, *12*, 1874; f) V. C. Nikolis, A. Mischok, B. Siegmund, J. Kublitski, X. K. Jia, J. Benduhn, U. Hormann, D. Neher, M. C. Gather, D. Spoltore, K. Vandewal, *Nat. Commun.* **2019**, *10*, 3706; g) N. Krainova, A. J. Grede, D. Tsokkou, N. Banerji, N. C. Giebink, *Phys. Rev. Lett.* **2020**, *124*, 177401.

[9] a) A. Canaguier-Durand, E. Devaux, J. George, Y. Pang, J. A. Hutchison, T. Schwartz, C. Genet, N. Wilhelms, J. M. Lehn, T. W.

Ebbesen, *Angew. Chem., Int. Ed.* **2013**, *52*, 10533; b) R. Houdre, R. P. Stanley, M. Ilegems, *Phys. Rev. A* **1996**, *53*, 2711; c) J. Mony, M. Hertzog, K. Kushwaha, K. Borjesson, *J. Phys. Chem. C* **2018**, *122*, 24917; d) T. Schwartz, J. A. Hutchison, J. Leonard, C. Genet, S. Haacke, T. W. Ebbesen, *ChemPhysChem* **2013**, *14*, 125; e) S. Wang, T. Chervy, J. George, J. A. Hutchison, C. Genet, T. W. Ebbesen, *J. Phys. Chem. Lett.* **2014**, *5*, 1433; f) B. Xiang, R. F. Ribeiro, L. Y. Chen, J. X. Wang, M. Du, O. E. Z. Yuen, W. Xiong, *J. Phys. Chem. A* **2019**, *123*, 5918; g) K. Yamashita, U. Huynh, J. Richter, L. Eyre, F. Deschler, A. Rao, K. Goto, T. Nishimura, T. Yamao, S. Hotta, H. Yanagi, M. Nakayama, R. H. Friend, *ACS Photonics* **2018**, *5*, 2182; h) R. T. Grant, P. Michetti, A. J. Musser, P. Gregoire, T. Virgili, E. Vella, M. Cavazzini, K. Georgiou, F. Galeotti, C. Clark, J. Clark, C. Silva, D. G. Lidzey, *Adv. Opt. Mater.* **2016**, *4*, 1615.

[10] a) M. Tavis, F. W. Cummings, *Phys. Rev.* **1968**, *170*, 379; b) M. Tavis, F. W. Cummings, *Phys. Rev.* **1969**, *188*, 692.

[11] a) V. M. Agranovich, M. Litinskaia, D. G. Lidzey, *Phys. Rev. B* **2003**, *67*, 085311; b) J. del Pino, J. Feist, F. J. Garcia-Vidal, *New J Phys* **2015**, *17*, 053040; c) M. Litinskaya, P. Reineker, V. M. Agranovich, *J. Lumin.* **2004**, *110*, 364; d) P. Michetti, G. C. La Rocca, *Phys. Rev. B* **2005**, *71*, 115320.

[12] L. Novotny, *Am. J. Phys.* **2010**, *78*, 1199.

[13] G. Groenhof, C. Climent, J. Feist, D. Morozov, J. J. Toppari, *J. Phys. Chem. Lett.* **2019**, *10*, 5476.

[14] B. E. Saleh, M. C. Teich, *Fundamentals of Photonics*, John Wiley & Sons, Hoboken, NJ, USA **2019**.

[15] G. D. Scholes, C. A. DelPo, B. Kudisch, *J. Phys. Chem. Lett.* **2020**, *11*, 6389.